ENGINEERING RESEARCH INSTITUTE
UNIVERSITY OF MICHIGAN
ANN ARBOR

EFFECTS OF SPACE-CHARGE ON FREQUENCY CHARACTERISTICS OF MAGNETRONS

Technical Report No. 4
Electron Tube Laboratory
Department of Electrical Engineering

By

H. W. WELCH, JR.

Approved by: W. G. DOW
G. HOK

Project M762

CONTRACT NO. W-36-039 sc-35561
SIGNAL CORPS, DEPARTMENT OF THE ARMY
DEPARTMENT OF ARMY PROJECT NO. 399-13-022
SIGNAL CORPS PROJECT NO. 112B-0

December, 1950

EFFECTS OF SPACE CHARGE ON FREQUENCY CHARACTERISTICS OF MAGNETRONS

BY

H. W. WELCH, JR.

Reprinted from the PROCEEDINGS OF THE I.R.E.
VOL. 38, NO. 12, DECEMBER, 1950

PRINTED IN THE U.S.A.

Effects of Space Charge on Frequency Characteristics of Magnetrons*

H. W. WELCH, JR.†, ASSOCIATE, IRE

Summary—**Properties of the magnetron space-charge swarm which affect the propagation of electromagnetic waves are defined in terms of an effective dielectric constant. The space charge is found to be doubly refractive in nature, the velocity of propagation depending on the direction of propagation of the wave, polarization of the wave, and frequency. Effects of synchronism of the rotating space-charge swarm are discussed qualitatively. Experimental results which check parts of the theory are presented. The relationship of the space charge to the circuit is discussed in terms of the nonoscillating and the oscillating magnetron.**

Introduction

THE COMPLETE DISCUSSION of space-charge effects on frequency characteristics of continuous-wave magnetrons requires attention to a varied subject matter. Much of this subject matter has been treated in reports of government agencies and in the journals, and is generally understood. There are, however, several points at which present knowledge becomes inadequate background for an understanding of the mechanism of magnetron operation. This is particularly the case when one is to predict quantitatively the behavior of magnetron space-charge clouds under the influence of radio-frequency fields.

The circuital aspects of magnetron frequency characteristics are generally treated by establishment of an equivalent circuit and interpretation of that equivalent circuit in terms of experimentally measurable quantities. The most conveniently measurable quantities are resonance wavelength, loaded Q, and minimum standing-wave ratio. The relationships between these quantities and other unmeasurable quantities in the equivalent circuit are fairly well defined and understood. This theory can be extended to explain semiquantitatively effects of the output circuit and load on magnetron frequency characteristics such as frequency pulling and long-line effect.

Frequency characteristics of an operating magnetron must be obtained from the following types of experimentally obtained information: Rieke diagrams, relating frequency of oscillation and power output to load characteristics; frequency pushing measurements, relating frequency and plate current for constant loading; and modulation characteristics determined by spectral measurements of various types. Interpretation of these types of data depends on knowledge of the physics of space-charge effects in the oscillating magnetron and, at this point, is almost entirely qualitative.

Another type of data, resulting from measurements made on magnetrons in which electrons are circulating but not reaching the anode, is very useful as an aid to the understanding of space-charge behavior. The method of measurement is the same as that used for cold impedance tests on microwave tubes and resonant cavities. In order to differentiate, the term "hot impedance test" is used, implying that the magnetron is "hot" and capable of drawing plate current if the conditions of anode voltage and magnetic field are proper adjusted.

In order to provide theoretical interpretation of the experimental results, it is necessary to study two types of properties of the space charge. These are the following:

Type 1—Properties having to do with the distribution of angular velocity, field, potential and charge density, and definition of the space-charge boundary in the magnetron interaction space.

Type 2—Properties having to do with the propagation of electromagnetic waves in the space-charge distribution defined by the results of the study of properties of Type 1.

The results of the study of properties of Type 1 will be presented when needed but not derived in this paper. The primary purpose will be the detailed discussion of properties of Type 2 and interpretation of the various effects of space charge on magnetron frequency characteristics. It will be pointed out that these effects result from three more-or-less separate phenomena which may occur together or separately. The picture is still incomplete experimentally, because of very large quantities of data which are necessary to survey the entire range of the variable parameters, and, theoretically, because of the complexity of parts of the necessary mathematical development. Another important factor is that, in most conventional magnetrons, the total effect of space charge on frequency is a shift of less than one or two per cent. A detailed study therefore requires a number of measurements accurate within at least 0.1 per cent.

The need for the study of space-charge effects on frequency characteristics lies in two directions. In the first place, it becomes possible for experimental results to provide a check on the basic theories of the magnetron space charge. In the second place, understanding of the use of the magnetron space charge in electronic frequency control or modulation is increased.

* Decimal classification: R138.1×R355.912.1. Original manuscript received by the Institute, October 10, 1949; revised manuscript received, May 25, 1950.

This paper is based on work done for the Signal Corps of the United States Army, under Contracts W36-039 sc-32245 and 36-039 sc-35561.

† Engineering Research Institute, University of Michigan, Ann Arbor, Mich.

The various conditions under which data may be taken give a wide range of possibilities for interpretation. In certain cases quantitative agreement between theory and experiment are obtained. The present paper is not meant to be a complete and final analysis of the problem of magnetron space-charge and frequency characteristics. It is intended to relate as many as possible of the known facts and theories in such a way that they can be used as a guide for further research and development. Gaps in both experimental data and theory will be pointed out with the hope that someone will have the necessary information, or the time to acquire the necessary information, to fill them in.

Formation of the Magnetron Space Charge

The static cylindrical magnetron space-charge distribution, which is often called the Hull or Brillouin solution, may be thought of as a swarm of electrons revolving around the cathode. This swarm is characterized by the condition that no radial current exists and by the following angular velocity distribution:

$$\omega = \frac{Be}{2m}\left(1 - \frac{r_c^2}{r^2}\right) \tag{1}$$

where

B = axially directed magnetic field
r_c = cathode radius
r = radius which locates electron
e = absolute value of electronic charge
m = electronic mass.

However, assuming no energy exchange with the surroundings, this distribution of angular velocity must exist in the static magnetron regardless of the radial velocity, initial or otherwise. If no radial velocity is present, then the corresponding potential distribution represents minimum energy of the electrons.

$$Ee = \frac{1}{2} m\left(\frac{Be}{2m}\right)^2 r^2\left(1 - \frac{r_c^2}{r^2}\right)^2 \tag{2}$$

where

E = electric potential.

If current is passed radially through the cloud, additional energy must be supplied which would add to the potential of the electrons given by (2). If the anode potential E_a is insufficient to supply the minimum energy at the anode (given by substituting the anode radius r_a into (2)), then the swarm of electrons must be bounded between cathode and anode. In order to calculate effects of the space charge under these conditions, the position of this boundary and the space-charge distribution within should be known. The position of the boundary is readily calculated because the potential and field at the swarm boundary are known. If no electrons are crossing the boundary, the potential at the boundary must be given by (2). The field is, therefore,

$$-\frac{\partial E}{\partial r} = \frac{1}{4}\frac{e}{m} B^2 r\left(\frac{r_c^4}{r^4} - 1\right). \tag{3}$$

By Gauss's theorem the total space charge per unit length within a radius r will be

$$\tau = 2\pi r\epsilon_0\left(-\frac{\partial E}{\partial r}\right) = \frac{1}{2}\pi\epsilon_0\frac{e}{m}B^2r^2\left(\frac{r_c^4}{r^4} - 1\right) \tag{4}$$

where

τ = total space charge per unit length
$\epsilon_0 = (1/36\pi)\times 10^{-9}$ farads per meter.

For a cylindrical diode

$$E_a - E = \frac{-\tau}{2\pi\epsilon_0}\log\frac{r_a}{r} \tag{5}$$

where

E_a = the anode potential
E = potential at some point in charge free space r
τ = charge per unit length inside r.

If we let

$r = r_H$ = boundary of space-charge swarm
$E = E_H$ = potential at r_H from (2)
τ = value defined by (4) for $r = r_H$,

and substitute from (2) and (4) into (5), we have

$$E_a = B^2\frac{e}{8m}r_H^2\left[2\left(1 - \frac{r_c^4}{r_H^4}\right)\log\frac{r_a}{r_H} + \left(1 - \frac{r_c^2}{r_H^2}\right)^2\right]. \tag{6}$$

This equation shows us that for a given magnetron, if E_a/B^2 is kept constant, the radius of the space-charge swarm remains constant (under static conditions).

It is important to note that in the derivation of (4) and (6) it was unnecessary to specify the distribution of space charge and potential inside the swarm. It is known that a number of solutions for these distributions are possible in which electrons stream back and forth between the cathode and the outer boundary of the space-charge swarm. Corresponding to each of these double-stream or multiple-stream solutions, as they are called, there would be a different potential and space-charge distribution within the swarm. All of these solutions have been obtained for the plane magnetron.[1] However, for the cylindrical magnetron the complete solution is not yet available. If it assumed that the solution is not multiple stream (i.e., that all of the electrons in the swarm are traveling in circles around the cathode), the resulting space-charge distribution is

[1] J. C. Slater, "Microwave Electronics," D. Van Nostrand Co., New York, N. Y., p. 336; 1950.

$$\rho = -\frac{1}{2}\epsilon_0 \frac{e}{m} B^2\left(1+\frac{r_c^4}{r^4}\right). \tag{7}$$

This is obtained by applying Poisson's equation to (3), and therefore corresponds to minimum energy in the electrons. This distribution will be used in the following discussion.

Propagation of the Electromagnetic Wave in the Magnetron Space Charge

The radio-frequency properties of the space charge have been analyzed previously in two important articles.[2,3] However, many points of particular interest to the problem of frequency characteristics have not been emphasized. In order to establish the relationship of the following treatment to the two previous treatments, the major differences will be pointed out. All three methods are alike in that the space-charge distribution given by (7) is the starting point, and, as was pointed out in the last section, there is no ambiguity in the use of (6) to determine the boundary of the space-charge swarm.

The fundamental equation of motion of an electron in space, in vector form, is

$$\frac{\vec{dv}}{dt} = -\frac{e}{m}(\vec{F} + \vec{v} \times \vec{B}) \tag{8}$$

where

$\vec{v}$ = velocity of the electron
$\vec{F}$ = electric field
$\vec{B}$ = magnetic field.

It is assumed that

$$\vec{v} = \vec{v}_0 + \vec{v}_1$$

$$\vec{F} = \vec{F}_0 + \vec{F}_1$$

$$\vec{B} = \vec{B}_0 + \vec{B}_1$$

where $\vec{B}_0$, $\vec{v}_0$, and $\vec{F}_0$ are static values and $\vec{B}_1$, $\vec{v}_1$, and $\vec{F}_1$ are impressed radio-frequency values. Substituting into (8) and keeping the terms involving radio-frequency values, we have

$$\frac{\vec{\partial v_1}}{\partial t} + (\vec{v}_0 \cdot \nabla)\vec{v}_1 + (\vec{v}_1 \nabla)\vec{v}_0 + (\vec{v}_1 \cdot \nabla)\vec{v}_1 = -\frac{e}{m}(\vec{F}_1 + \vec{v}_1 \times \vec{B}_0 + \vec{v}_0 \times \vec{B}_1) \tag{9}$$

where we are following the motion of a particular electron. The left side is the total derivative $\vec{dv}/dt$ under these conditions. It is generally agreed that the term $\vec{v}_0 \times \vec{B}_1$ is negligible compared to other terms. In the paper by Blewett and Ramo the term $\vec{v}_1 \times \vec{B}_0$ is also neglected. Actually the effect of the magnetic field is quite important, as will be shown in the following, and as was also pointed out by Lamb and Phillips.

In the paper by Lamb and Phillips it was assumed that v_1 was a small perturbation and therefore the term $(\vec{v}_1 \cdot \nabla)\vec{v}_1$ could be neglected. Their results apply particularly to frequencies near the cyclotron frequency

$$\left(f_c = \frac{1}{2\pi}\frac{Be}{m}\right)$$

and are limited to very small sheaths of electrons surrounding the cathode. Damping is treated in a qualitative sense. Their results will be discussed further at the end of this section.

In the present approach, a simplified problem is treated in order to obtain more generally applicable results. These results will indicate an approximate behavior to be expected in a magnetron which seems to check closely enough with experimental observations to justify the method of treatment. It is assumed that the space-charge swarm is moving with a uniform velocity v_0 so that the term $\vec{v}_1 \cdot \nabla\vec{v}_0$ is dropped in (9). Actually

$$v_0 = \omega r = \frac{Be}{2m} r\left(1 - \frac{r_c^2}{r^2}\right),$$

from (1). Also, the wave is assumed to be propagated perpendicular to $\vec{v}_0$ so that the product $\vec{v}_0 \cdot \nabla\vec{v}_1$ vanishes. The force equation under these conditions becomes simply

$$\frac{\vec{\partial v_1}}{\partial t} = -\frac{e}{m}(\vec{F}_1 + \vec{v}_1 \times \vec{B}) \tag{10}$$

where the subscripts "1" only serve to indicate radio-frequency values and will be dropped in the remainder of the discussion.

Ordinarily in treatment of electrodynamics of a moving medium the effect of the motion does not become appreciable until the velocity is an appreciable fraction of the velocity of light. In the case of the magnetron, however, the effect of the motion may become important when the angular velocity of the edge of the swarm approaches synchronism with the angular velocity of the radio-frequency wave in the interaction space. Under these conditions the electrons can contribute energy to the radio-frequency wave and begin to slow down and form spokes extending toward the anode. These spokes assume a certain phase relationship to the radio-frequency wave which changes with plate voltage and affects frequency in a way not covered by the treatment in this section. Thus the results of this section should only be considered valid for

$$\omega \ll \omega_n \tag{11}$$

[2] J. P. Blewett and S. Ramo, "High frequency behavior of a space charge rotating in magnetic field," *Phys. Rev.*, vol. 57, pp. 635–641; April, 1940.

[3] W. E. Lamb, Jr., and M. Phillips, "Space charge frequency dependence of magnetron cavity," *Jour. Appl. Phys.*, vol. 18, pp. 230–238; February, 1947.

where

$\omega_n = 2\pi f/n$ (synchronous angular velocity)
f = frequency of the radio frequency impressed on the magnetron structure
n = mode number = $\frac{1}{2}$ number of anodes in π mode.

Since we are considering the space charge as an atmosphere of determined density and boundary, it is immaterial what system of co-ordinates is used for the force equation. We are considering properties of space-charge atmosphere as they affect propagation, so it will be simpler to treat a plane wave. The results will then be interpreted in the case of the particular geometry of the magnetron. We will assume first a configuration as shown in Fig. 1(a). Magnetic field is oriented in the z direction; a plane wave is propagated in the x direction. Fig. 1(b) shows, in comparison, the actual case in a magnetron. The force equations and Maxwell's equations yield the following:

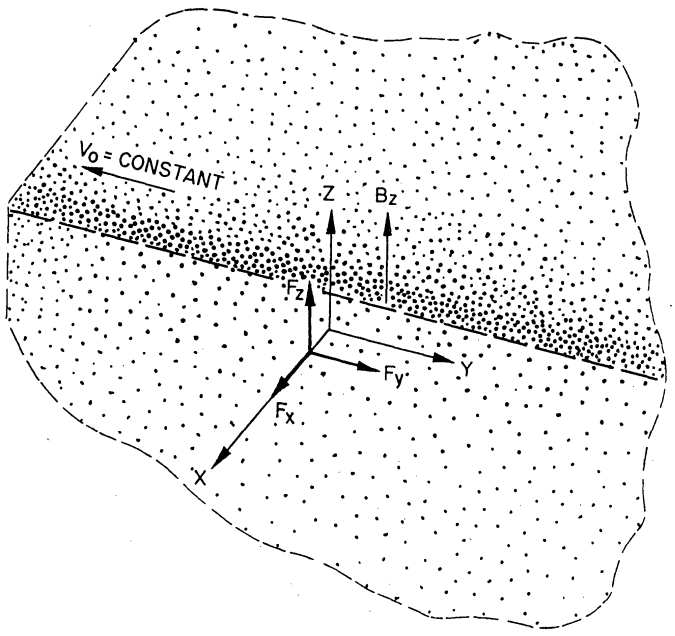

(a)

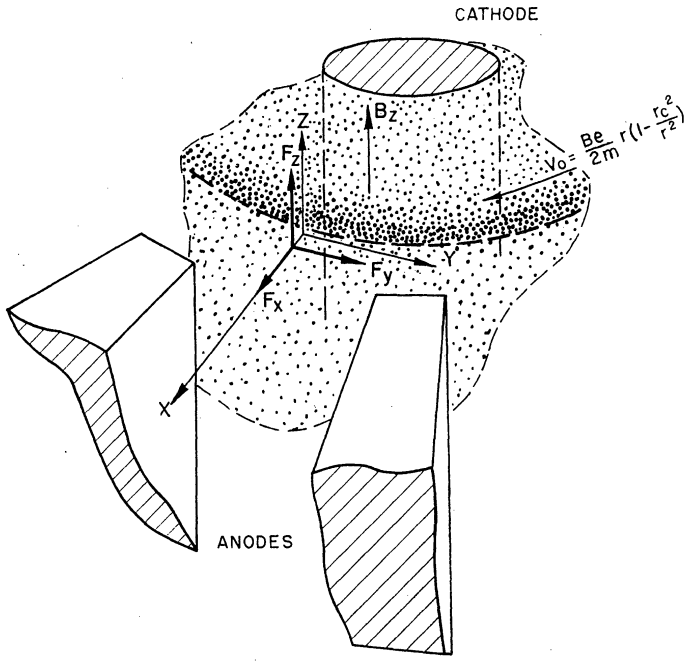

(b)

Fig. 1—(a) Orientation of field vectors assumed for development of equation (22); space-charge swarm moving with uniform velocity. (b) Orientation of field vectors in magnetron space charge.

$$\ddot{x} + \frac{e}{m}F_x + \omega_c\dot{y} = 0 \tag{12}$$

$$\ddot{y} + \frac{e}{m}F_y - \omega_c\dot{x} = 0 \tag{13}$$

$$\ddot{z} + \frac{e}{m}F_z = 0 \tag{14}$$

$$\epsilon_0\frac{\partial F_x}{\partial t} + \rho\dot{x} = 0 \tag{15}$$

$$\frac{\partial H_z}{\partial x} + \epsilon_0\frac{\partial F_y}{\partial t} + \rho\dot{y} = 0 \tag{16}$$

$$\frac{\partial H_y}{\partial x} - \epsilon_0\frac{\partial F_z}{\partial t} - \rho\dot{z} = 0 \tag{17}$$

$$\frac{\partial H_x}{\partial t} = 0 \tag{18}$$

$$\frac{\partial F_y}{\partial x} + \mu_0\frac{\partial H_z}{\partial t} = 0 \tag{19}$$

$$\frac{-\partial F_z}{\partial x} + \mu_0\frac{\partial H_y}{\partial t} = 0 \tag{20}$$

$\omega_c = B\dfrac{e}{m}$ B is z-directed steady magnetic field.

A solution of the type $Ae^{i(kx\pm\omega_f t)}$ is assumed for each of the quantities x, y, z, F_x, F_y, F_z, H_x, H_y, and H_z. ($\omega_f = 2\pi f$). A different constant A, of course, is used in each case. Substituting in (12) through (20) and differentiating, a set of simultaneous equations is obtained. The determinant of the coefficients in these equations is the following

x	y	z	F_x	F_y	F_z	H_y	H_z
$-\omega_f^2$	$\pm i\omega_f\omega_c$	0	e/m	0	0	0	0
$\mp i\omega_f\omega_c$	$-\omega_f^2$	0	0	e/m	0	0	0
0	0	$-\omega_f^2$	0	0	e/m	0	0
$\pm\rho$	0	0	$\pm\epsilon_0$	0	0	0	0
0	$\pm\rho$	0	0	$\pm\epsilon_0$	0	0	$+k/\omega_f$
0	0	$\pm\rho$	0	0	$\pm\epsilon_0$	$-k/\omega_f$	0
0	0	0	0	$+k/\omega_f$	0	0	$\pm\mu_0$
0	0	0	0	0	$-k/\omega_f$	$\pm\mu_0$	0

By Cramer's rule, in order for a solution other than a trivial solution to exist this determinant must be identically equal to zero.[4] It is convenient to solve for $k^2/\epsilon_0\mu_0\omega_f^2 = c^2/v^2$ where c = velocity of light and v = phase velocity of the wave. c/v is the effective index of refrac-

[4] See any advanced calculus text for discussion of this rule.

tion of the medium and c^2/v^2 therefore the effective relative dielectric constant ϵ_r. The result is

$$\epsilon_r = 1 + \frac{\rho e}{\epsilon_0 m} \frac{\left(\omega_f^2 + \frac{\rho}{\omega_0}\frac{e}{m}\right) - 1/2\omega_c^2(1 \mp 1)}{\omega_f^2\left(\omega_f^2 - \omega_c^2 + \rho\frac{e}{m}\right)} \cdot \quad (21)^5$$

From (7) the space-charge density in a magnetron at the boundary of a swarm of radius r is

$$\frac{\rho e}{\epsilon_0 m} = -1/2\omega_c^2\left[1 + \left(\frac{r_c}{r}\right)^4\right] \quad (7a)$$

Letting

$$1 + \left(\frac{r_c}{r}\right)^4 = M,$$

the complete result for effective dielectric constant of the magnetron-type space charge may be written

$$\epsilon_r = 1 - \frac{M}{2}\frac{\omega_c^2}{\omega_f^2}\frac{\omega_f^2 - 1/2(M + 1 \mp 1)\omega_c^2}{\omega_f^2 - \omega_c^2\left(1 + \frac{M}{2}\right)} \cdot \quad (22)$$

For the $(-)$ sign

$$\epsilon_r = 1 - \frac{M}{2}\frac{\omega_c^2}{\omega_f^2}\frac{\frac{\omega_f^2}{\omega_c^2} - \frac{M}{2}}{\frac{\omega_f^2}{\omega_c^2} - \left(1 + \frac{M}{2}\right)} \cdot \quad (23)$$

For the $(+)$ sign

$$\epsilon_r = 1 - \frac{M}{2}\frac{\omega_c^2}{\omega_f^2} \cdot \quad (24)$$

The result of (24) is exactly the same as the result which is obtained when no steady magnetic field is assumed present and is the result obtained in the paper by Blewett and Ramo, due to the neglect of the cross product of the radio-frequency velocity and the static magnetic field in the force equation.

Another case should be mentioned, which, although it does not occur in the conventional magnetron, is of importance in some structures which use the magnetron-type space charge to vary reactance for electronic frequency modulation. In this case the direction of wave propagation is assumed parallel to the direction of the magnetic field. This case is treated by the same method as the one just treated with the result

$$\epsilon_r = 1 - \frac{M}{2}\frac{\omega_c}{\omega_f}\frac{1}{\frac{\omega_f}{\omega_c} \pm 1} \cdot \quad (25)^6$$

[5] It should be noted that the $(\pm)$ sign in this result is not a result of the assumption of a $(\pm)$ sign in the assumed solution but results from the quadratic nature of the solution of the determinant.

[6] In this case the $(\pm)$ sign is a result of the assumption that it exists in the exponential solution.

Equations (22) and (25) are plotted in Figs. 2(a) and 2(b) with the assumption that $M=1$. This is approximately true only for values of r_c/r less than 1/3. The curves as plotted will, however, represent the picture with sufficient accuracy to support discussion.

The meaning of each of the various values of effective dielectric constant is not obvious from the development presented here. However, further examination of the polarizations of the waves and of a physical picture show the following to be true.

In Fig. 2(a) the solid curve from (23) corresponds to an electromagnetic wave polarized with the E vector perpendicular to the static magnetic field. The wave cannot be entirely transverse because there must be a component of E in the direction of propagation. The actual situation in an ideal multianode magnetron

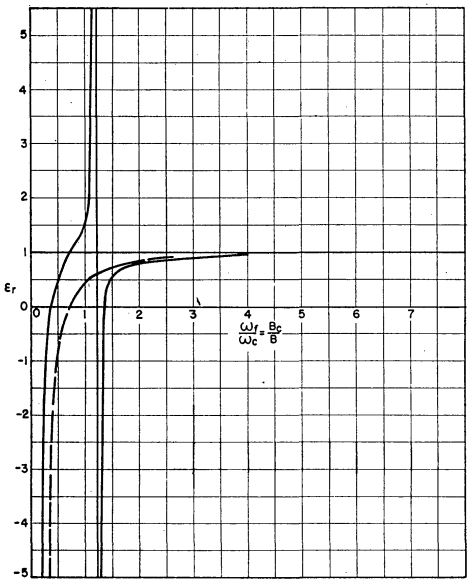

(a)

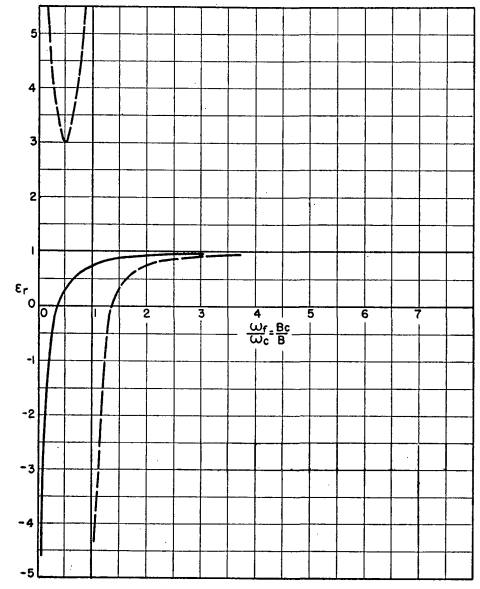

(b)

Fig. 2—Dielectric constant of magnetron space charge as function of $\omega_f/\omega_c = B_c/B$. (a) Direction of propagation transverse to direction of magnetic field. (b) Direction of propagation same as direction of magnetic field.

should be approximated by this case as examination of Fig. 1(b) will show. If end effects are neglected, the electric fields are entirely in the xy plane perpendicular to the static magnetic field. However, propagation is not always perpendicular to $\vec{v_0}$.

In Fig. 2(a) the dotted curve from (24) corresponds to an electromagnetic wave polarized with the E vector parallel to the static magnetic field. In this case the presence of the magnetic field does not have any effect, as was pointed out previously.

In Fig. 2(b) the solid curve from (25) with + sign corresponds to an electromagnetic wave with left-hand circular polarization.

In Fig. 2(b) the dotted curve from (25) with − sign corresponds to an electromagnetic wave with right-hand circular polarization.

The effective dielectric constant, which is really a measure of phase velocity of the wave, depends on polarization, relationship of direction of propagation to direction of magnetic field, and value of ω_f/ω_c. The properties of these regions and the effect to be expected in a magnetron-type structure may be summarized as follows:

$\epsilon_r<0$. In this case the phase velocity is imaginary; a wave will not propagate within the space charge; therefore, a space-charge boundary acts as a reflecting surface. The capacitance between cathode and anodes is increased by the presence of the space charge.

$0<\epsilon_r<1$. In this case the phase velocity of the wave exceeds the velocity of light. The capacitance between cathode and anodes is decreased by the presence of space charge.

$\epsilon_r>1$. In this case the phase velocity of the wave is less than the velocity of light. The capacitance between cathode and anodes is increased by the presence of the space charge.

The total range of values covered by the graphs of Fig. 2 represents a considerable variation of conditions which might be imposed on the magnetron-type structure. Data exist only in limited regions; some of this will be presented in the next section.

It will be interesting at this point to compare these results with the results of Lamb and Phillips. In their paper the behavior near the cyclotron resonance is described from an impedance point of view for very small sheaths of electrons surrounding the cathode. This result is the following:

$$Z_{el} \cong \frac{F_\theta}{H} = \frac{in^2 s}{r_c^2 \epsilon_0 \omega_f} \frac{\omega_f^2}{\omega_c^2 - \omega_f^2} \tag{26}$$

where

F_θ/H = the ratio of the electric field vector to the magnetic field vector

s = thickness of the electron sheath around the cathode.

It is assumed that

$$\frac{ns}{r_c} < \frac{\omega_c^2 - \omega_f^2}{\omega_f^2} \quad \text{and} \quad n \neq 0.$$

This restriction on the magnitude of s/r_c is a severe limitation in the practical case of an oscillating magnetron or frequency-modulation structure. In either of these cases, s/r_c can be an appreciable fraction of r_a/r_c. An effective cathode radius may be calculated which, when used as a boundary condition, obtains the same effect on resonant frequency of the anode block as the condition of (26). Thus

$$r_{ceff} = r_c\left(1 + \frac{2ns}{r_c} \frac{\omega_f^2}{\omega_c^2 - \omega_f^2}\right)\frac{n}{2}. \tag{27}$$

This result predicts a resonance at the cyclotron frequency which is qualitatively described by a positive wavelength shift (capacitance increase) for $\omega_f/\omega_c<1$ and a negative wavelength shift (capacitance decrease) for $\omega_f/\omega_c>1$. This effect and the type of effects predicted by (23) might be simultaneously possible in an actual magnetron, since the assumptions involved in neither development can be held except in extreme cases. A qualitative picture of the behavior of the electrons near the cyclotron resonance is given in Fig. 3. In all cases the angular frequency impressed on the anode is assumed to be the cyclotron frequency. ω is the angular velocity of the outermost electrons. If

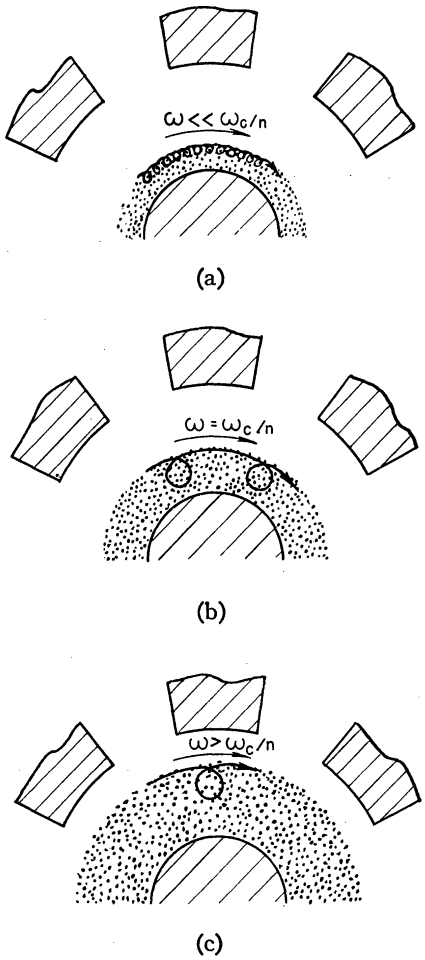

Fig. 3—Qualitative picture of cyclotron resonance.

$\omega \ll \omega_c/n$ (corresponding to small s), as in Fig. 3(a), the perturbed electron will execute several cycles in passing a set of anodes. In this case the resonance effect should occur very near the cyclotron frequency. The effect of the steady-state angular velocity is not important. If $\omega = \omega_c/n$, as in Fig. 3(b), the electron executes a single cycle in just the time it takes it to move, due to the steady-state velocity, from one set of anodes to the next. In the same time, the direction of the field between the next set of anodes has changed to be in phase with the electron oscillation. In the case of Fig. 3(c), the electron does not execute a single cycle in transit between two anodes and arrives between the next set out of phase with the field. Essentially these observations mean that the magnetic field for the cyclotron resonance should be a function of voltage. This has been observed experimentally and is presented in Fig. 10. To our knowledge more extensive data on the cyclotron resonance which might serve to clarify the picture do not exist.

Space Charge and the Equivalent Circuit

The details of an equivalent circuit for a microwave device such as a magnetron naturally change with the structure of the magnetron. Effects of end hats, straps supporting structures, and the like may or may not be important enough to be included in the circuit. The equivalent circuit is usually based on the assumption that the various possible modes of oscillation are sufficiently separated in frequency to be considered individually. This permits the representation of the resonant circuit of the magnetron as a simple parallel resonant circuit. When this assumption is not valid, the resonance is made complex and, in general, must be treated as a special case. However, if the assumption is not justified, some sort of device is usually necessary to induce mode separation before the magnetron is practically usable. Thus, in most practical cases the simplified approach is adequate.

The most important concept in connection with equivalent circuits of magnetrons relative to the present problem is the concept of electron-transit admittance. It is the susceptive portion of this admittance which affects frequency characteristics of the magnetron. If an equivalent circuit may be established in which the function of the electron-transit susceptance is properly understood, the picture is greatly simplified. This has been done with satisfactory results for triodes, tetrodes and klystrons, but the picture in the case of magnetrons is still obscure. The circuit in Fig. 4(a) is suggested as equivalent in the case of a nonoscillating magnetron. In this circuit, the electron-transit admittance is represented by y_e which may be defined as the admittance of the electrons as seen from terminals representing the two sets of anodes. The nature of this admittance changes for various conditions of anode voltage, magnetic field, and radio-frequency voltage between anode segments. The primary purpose of this paper is to present the over-all picture of these changes. The picture for an oscillating magnetron is more complex. However, a convenient picture is obtained by replacing the admittance y_e by a current generator $i_g = y_e e_T$ (see Fig. 4(b)). The admittance y_e may now be thought of as the equivalent admittance of a current generator. The value of this admittance is a function of plate current and loading. Variation in the susceptive portion of this admittance with current is the cause of frequency pushing. This will be discussed in a following section.

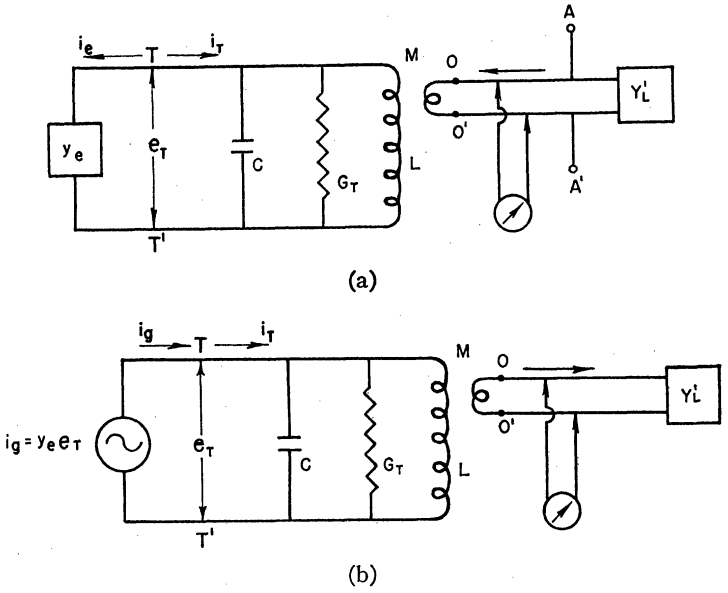

Fig. 4—Equivalent circuits; arrow indicates direction of power flow. (a) Equivalent circuit for nonoscillating magnetron. (b) Equivalent circuit for oscillating magnetron.

Experimental investigation of the nature of the quantity y_e must be made by a meter located in the line between the output terminals O and O' and the load Y_L. In the case of the nonoscillating magnetron (Fig. 4(a)) an external signal must be fed into the circuit at the points A and A'. Measurements of standing-wave ratio and position of minimum, coupled with a knowledge of properties of the circuit and the controllable parameters in the circuit, yield an experimental result for y_e as a function of the variable parameters. This type of measurement we call a hot impedance test, in analogy with the established term, cold impedance test. When anode voltage is increased to the point of supporting oscillation, these measurements can no longer be made and the circuit in Fig. 4(b) applies. Standing-wave ratio and position of the minimum measurements now apply to the load. No external source is present. The load is therefore used as a variable and the effect on resonant wavelength, power output, and the like is recorded in the Rieke diagram. Variation of frequency with the plate current (frequency pushing) can be measured quite simply in connection with over-all performance data taken for constant loading.

In the case of the nonoscillating tube, a radio-frequency voltage may be considered applied across the

capacitive portion of the magnetron circuit, at the boundary between the resonant circuit structure and the interaction space. This is represented by T–T' in Fig. 4(a). The radio-frequency voltage causes a current i_T to flow into the tank circuit. If there are electrons present in the interaction space they may be represented by an admittance y_e through which a current i_e will flow. The currents i_e and i_T are independent of each other if the radio-frequency voltage is assumed unaffected by their magnitudes. If the admittance of the tank circuit is known, the admittance y_e could presumably be measured. This admittance should be dependent upon the values of magnetic field, anode voltage, radio-frequency voltage, and geometry of the interaction space.

In the case of the oscillating magnetron as represented in Fig. 4(b), the current i_T, developed in the tank circuit, is induced by spokes of synchronous space charge rotating in the interaction space. This current results in a radio-frequency voltage at the terminals T–T'. The current cannot exist until the oscillations become regenerative. The synchronous space-charge spokes cannot exist until radio-frequency voltages are present, i.e., until oscillation starts. The rotating spokes of synchronous space charge may be thought of as a current generator. There is a phase difference between the generated current and the radio-frequency voltage which causes the oscillations to build up at a lower frequency than the natural resonance frequency of the tank circuit. This phase difference and the equivalent negative conductance of the electrons are represented in y_e, the admittance equivalent to the generator representing the electrons. The value of this admittance must be such that the net susceptance and conductance of the circuit are cancelled at the frequency of oscillation. When the admittance characteristic of the tank circuit is known as a function of frequency near resonance, the value of y_e can be calculated.

These two interpretations of y_e should be kept in mind while reading the following sections. We will find that in the first case for the nonoscillating magnetron, the space-charge effects on frequency are primarily a function of the dimensions and density of the hub of the space-charge wheel. (See Fig. 13 for pictorial representation of the space charge.) In the second case of the oscillating magnetron, the effect on frequency is due to the phase relation of the spokes of synchronous space charge to the radio-frequency voltage. The two effects may cause frequency shifts in opposite directions. Quantitative agreement between experiment and theory for the first case is shown in the Appendix. In the second case, only qualitative discussion is thus far possible.

Space-Charge Effects in the Nonoscillating Magnetron

In order to measure effects of space charge in the nonoscillating magnetron, hot impedance measurements must be made from the output terminals. The measurements which have been taken are of four types as follows:

1. Impedance measurements at constant magnetic field and radio-frequency voltage, anode potential as variable parameter.
2. Impedance measurements at constant magnetic field and anode potential, radio-frequency voltage as variable parameter.
3. Resonant wavelength measurements at low radio-frequency voltage for different magnetic fields, anode potential as variable parameter.
4. Resonant wavelength measurements at low radio-frequency voltage and constant space-charge swarm radius, magnetic field as variable parameter.

A schematic drawing of the experimental setup is shown in Fig. 5. In order to obtain high radio-frequency voltage, one magnetron is used to drive another. Radio-frequency voltage is varied by means of attenuating reflectors placed in a slotted section between

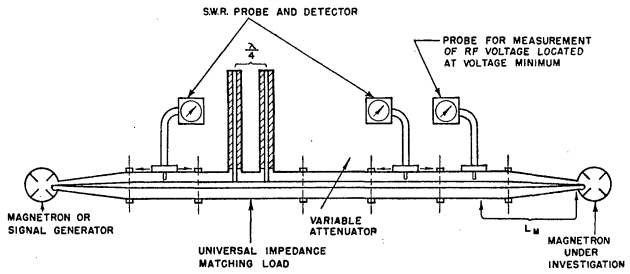

Fig. 5—Experimental apparatus for hot impedance heating.

the impedance matching load and the magnetron under investigation. Radio-frequency voltage is measured by a probe placed at a voltage minimum (at cold resonance) approximately three wavelengths from the magnetron coupling loop (L_M in the diagram). This probe leads to a crystal detector and microammeter. The probe is calibrated against power measurements into a matched load and radio-frequency voltage calculated from the known line impedance of 52 ohms. The impedance matching load is quite useful for measurements of this type or in any application where a high-Q circuit is to be driven by a magnetron. It consists of two loads separated by $\lambda/4$. The driving magnetron is thus under no circumstances subject to standing-wave ratios greater than three to one.

In the impedance measurements, Q_0, λ_0 and G_0 are measured and plotted against the variable parameter, Q_0 is the unloaded Q of the magnetron, λ_0 is the resonant wavelength, and G_0 is the input conductance at resonance. $G_0 = Y_0/\sigma_0$, where σ_0 is the minimum standing-wave ratio and Y_0 is the characteristic admittance of the line.

The results of hot impedance measurements made under various conditions are shown in Figs. 6 through 12. The results shown in Fig. 6 offer a comparison between frequency effects in the nonoscillating magnetron and in the oscillating magnetron. The increasing reso-

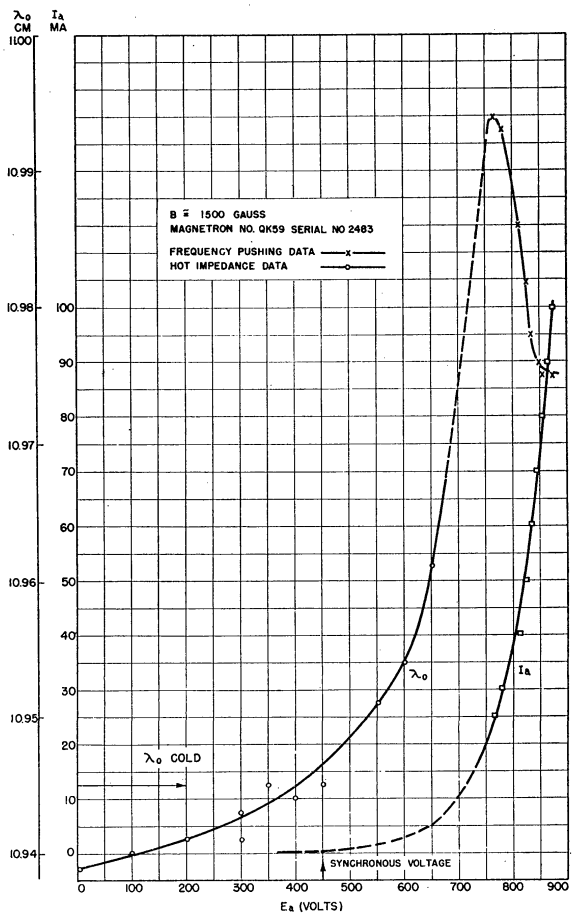

Fig. 6—Change of magnetron resonant wavelength with plate voltage. Comparison of frequency pushing and hot impedance test results.

nant wavelength up to the voltage for which synchronism begins (450 volts) is due to the capacitance between anodes increasing as a cloud of electrons of negative dielectric constant expands within the anode structure. This is what may be called a passive effect of the electrons. Above this point synchronous reactance causes a sharp rise in wavelength, and when oscillation starts the direction of wavelength shift reverses. The original cold resonant wavelength is not reached. This reversal effect is called frequency pushing, and may be called an active effect of the electrons. Frequency pushing and synchronous reactance will be discussed qualitatively in the next section. The passive effects in the preoscillating region can be discussed more quantitatively. This is done in the Appendix in terms of the data on tubes built in the Michigan laboratory.

In Fig. 7 the variation of λ_0, Q_0 and G_0 is plotted against plate voltage for two values of radio-frequency voltage impressed upon the anode structure. The general form of the curves is seen to be the same, with a reduction in Q as the radio-frequency voltage is raised. The Q_0 curves are relatively flat up to about 700 volts. This indicates that there is no change in the conductive characteristics of the space charge in this region. At about 700 volts, the Q_0 begins to rise sharply. At the point of oscillation it would, ideally, go to infinity as the conductance goes to zero. This point occurs at about 900 volts. This behavior means that in the region between 700 and 900 volts space charge is contributing energy to the radio-frequency field and therefore synchronous bunches of space charge have been formed. When the Q_0 curve intersects with the cold Q_0 line the space charge is contributing just enough negative conductance to compensate for losses which may be present within the space charge due to bombardment of the cathode and collisions with large ions. The further increase in Q_0 represents compensation for copper losses in the resonant circuit. The reduction of the Q_0 in the flat portion of the curve is due to increase in losses due to back bombardment as radio-frequency voltage is raised. The data in Fig. 8 show how the Q_0 varies with radio-frequency voltage for a value of anode voltage in the flat portion of the curve of Fig. 7. The losses are

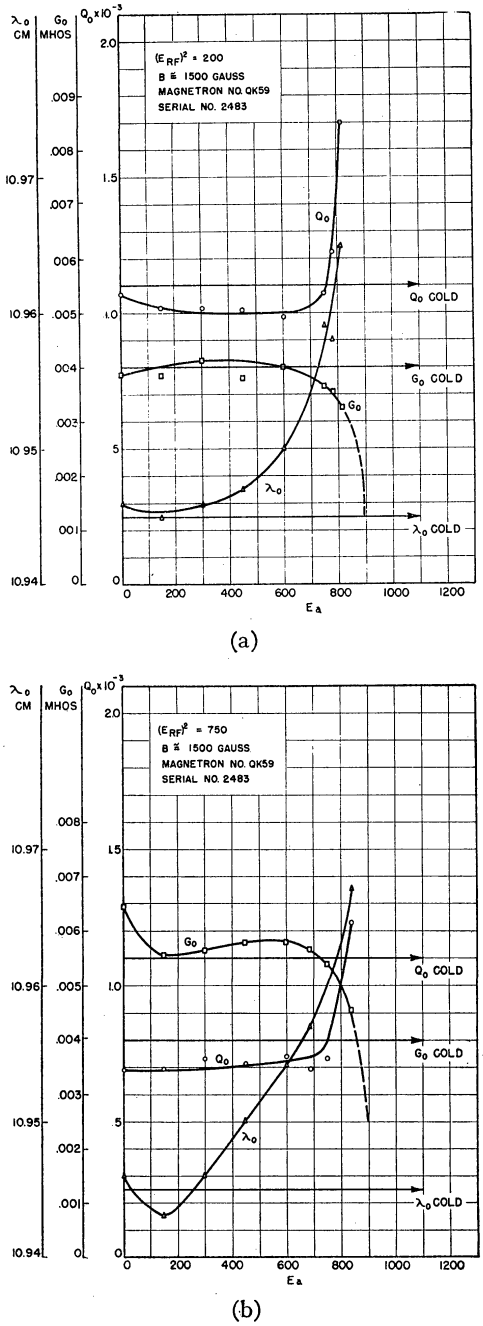

Fig. 7—Q_0, λ_0, and G_0 of hot magnetron as a function of plate voltage for various radio-frequency voltages.

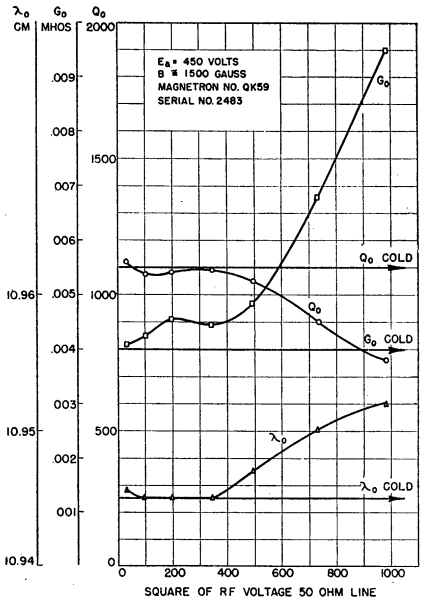

Fig. 8—Q_0, λ_0, and G_0 of hot magnetron as function of radio-frequency voltage for constant plate voltage.

going up rather rapidly with the increasing radio-frequency voltage. This is probably due to an increase in the energy spent in back bombardment of the cathode.

The complexity of the space-charge frequency characteristics in the nonoscillating magnetron when a wide range of variables is considered is clearly illustrated by the four sets of data in Fig. 9. These data were taken by an absorption method in which resonance was observed on an oscilloscope pattern. Q measurements could not be made. The radio-frequency voltage was supplied from a klystron signal source. The curves are similar to those just discussed except that E/B^2 is used as the independent variable. The radius of the space-charge swarm, in the absence of radio frequency, is proportional to this quantity. In the presence of radio frequency there are three critical conditions involving magnetic field and voltage; these are expressed by (28), (29), and (30) which follow. The critical values are noted on the curves of Fig. 9.

$$\omega_c \cong \frac{B_c e}{m} \tag{28}$$

where

$$\omega_c = \frac{2\pi c}{\lambda_c}$$

c = velocity of light.

This equation defines the cyclotron resonance. λ_c is the critical wavelength for the particular magnetic field B_c at which the period of natural rotation of an individual electron in the magnetic field is equal to the period of the radio-frequency cycle. As was pointed out in the discussion of Fig. 3 the resonance in the magnetron space charge should also be a function of voltage. This is borne out in the results shown in Figs. 9(b)

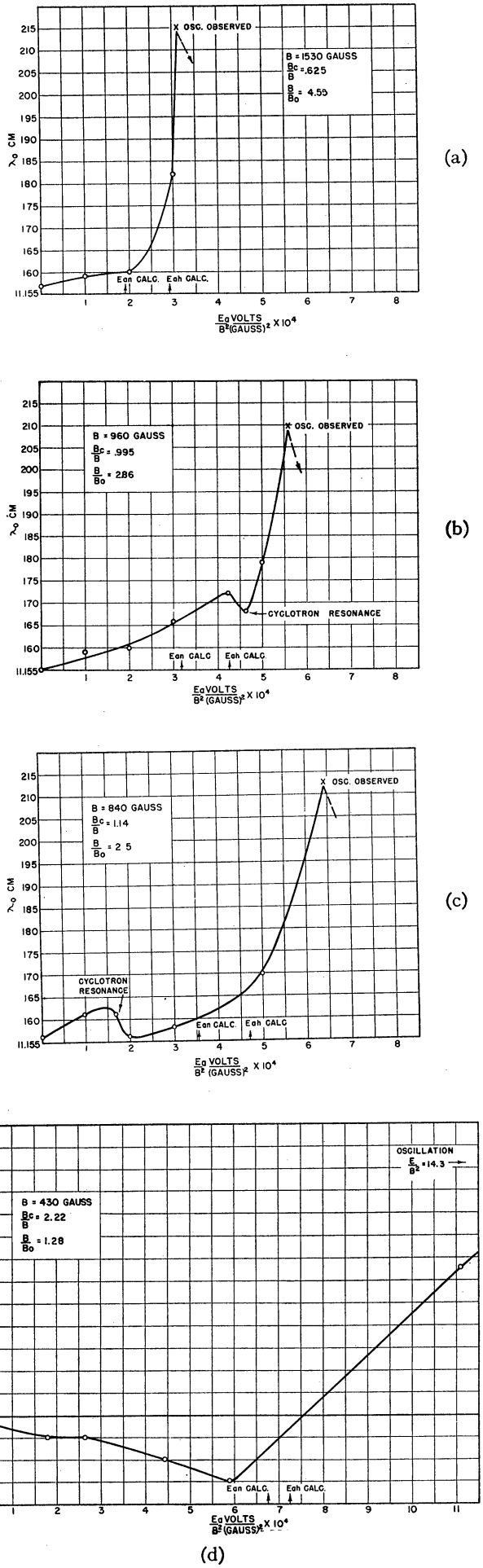

Fig. 9—Hot impedance test on QK59 no. 2483.

and 9(c) where the cyclotron resonance shows up as a perturbation of the resonant wavelength for two different voltages at slightly different magnetic fields.

chronous electrons can reach the anode with no radially directed velocities (Hartree voltage). This voltage is approximately the voltage at which oscillations begin.

$$\frac{E_{an}}{E_0} = \frac{B_n}{B_0} \frac{r_c^2/r_a^2}{\frac{B_n}{B_0} - \left(1 - \frac{r_c^2}{r_a^2}\right)} \left[2 \left(\frac{B_n}{B_0} \frac{2}{1 - \frac{r_c^2}{r_a^2}} - 1 \right) \log \frac{\sqrt{\frac{B_n}{B_0} - \left(1 - \frac{r_c^2}{r_a^2}\right)}}{\frac{r_c}{r_a}\sqrt{\frac{B_n}{B_0}}} + 1 \right] \tag{29}$$

where

$$E_0 = \frac{m}{2e} \omega_n^2 r_a^2$$

$$B_0 = \frac{2m}{c} \omega_n \frac{1}{(1 - r_c^2/r_a^2)}$$

(ω_n defined in (11)).

Equation (29) relates the anode voltage (E_{an}) and magnetic field (B_n) for which outer electrons in the space-charge swarm reach a velocity synchronous with the angular velocity of the radio-frequency wave traveling around the interaction space. For higher voltages than E_{an} the electrons are trying to move faster than synchronism and can give energy to the radio-frequency field. This condition shows up as a contribution of negative conductance and positive susceptance to the system, thus causing a rather sharp increase in Q and resonant wavelength.

$$\frac{E_{ah}}{E_0} = 2\frac{B}{B_0} - 1. \tag{30}$$

This equation defines the anode voltage at which syn-

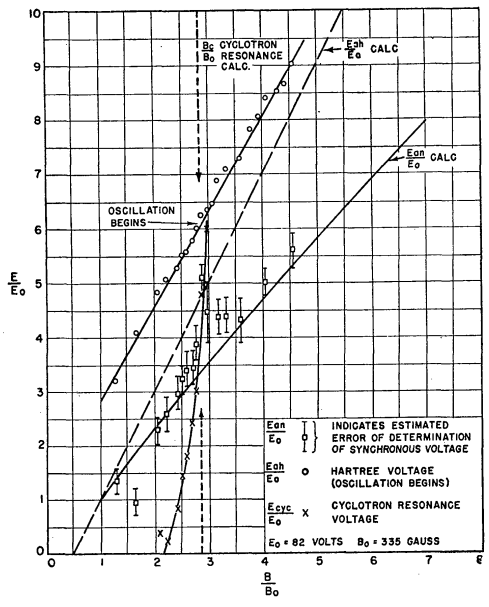

Fig. 10—Summary data on QK59 no. 2483 illustrating equations (28), (29), and (30).

Fig. 10 presents summary data of these three conditions extracted from a group of 26 curves similar to those of Fig. 9. The calculated values are presented for comparison. A considerable spread is represented for points on the curve for E_{an}/E_0, since the point at which a sudden increase in resonant wavelength occurs on the experimental curves is not definite.

The observed starting voltage seems to bear a definite relation to the calculated Hartree voltage, since the slopes of the two curves are approximately the same. The difference is probably due to the effect of the load on the starting voltage. This has not been quantitatively analyzed, but it may be said that, in a given magnetron, as the Q is lowered the starting voltage is raised.

The critical magnetic field for the cyclotron resonance is quite obviously affected by voltage. No satisfactory theory has been developed to give quantitative explanation of this effect. The synchronous voltage checks very well, considering the region of doubt which exists in its determination. It seems to be strongly perturbed in the region of the cyclotron resonance. It is interesting to note, however, that the cyclotron resonance seems to have no particular effect on the starting voltage for oscillation.

The static cutoff voltage (given by (2) with $r = r_a$) is calculated to be $E/B^2 = 7.4$. It is quite obvious in Fig. 9(d) and several other sets of data which are not given that this is not checked for low magnetic field in this particular magnetron.

In order to observe effects on resonant frequency due only to the change in effective dielectric constant of the space-charge swarm (as given by (23)), it is necessary to use data taken at various magnetic fields and at constant swarm radius. It is also necessary to stay below the voltage required to produce synchronous electrons. Thus, data in the curves of Fig. 9 taken below the synchronous voltage should represent the effect due to to the expansion of a space-charge swarm having an effective dielectric constant determined by $B_c/B = \omega_f/\omega_c$. Wavelength shift for four values of E/B^2 and varying B is plotted in Fig. 11. The position of the observed cyclotron resonance and the calculated field required for synchronism are marked. The latter is given by

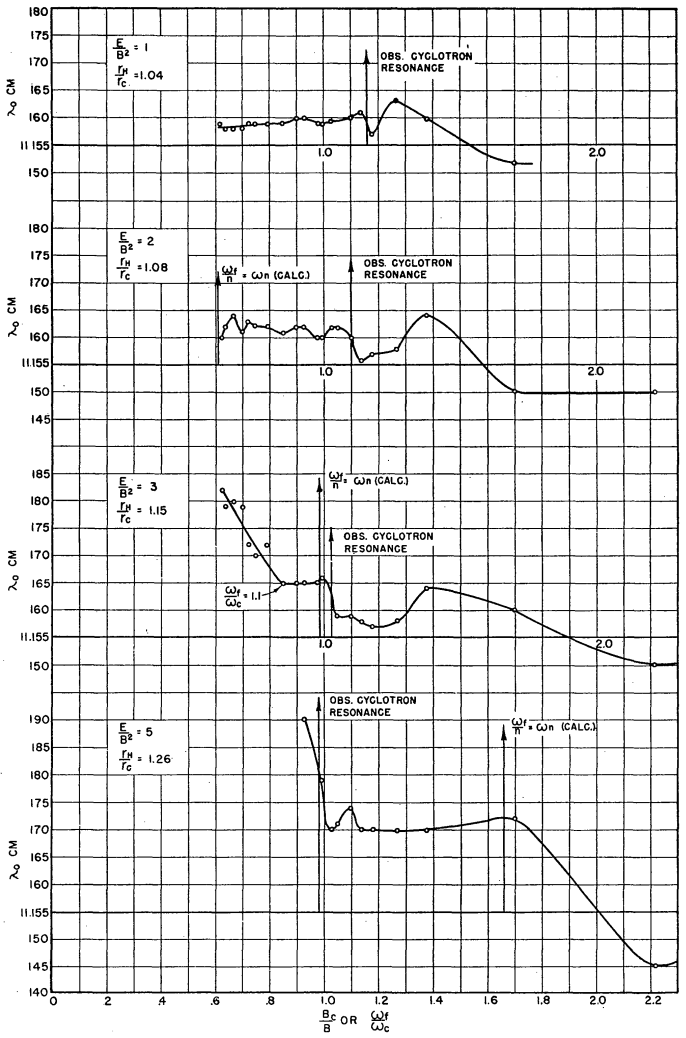

Fig. 11—Hot impedance test on QK59 no. 2483.

$$\frac{B_n}{B_0} = \frac{1 - \dfrac{r_c^2}{r_a^2}}{1 - \dfrac{r_c^2}{r_n^2}}. \qquad (31)$$

For $\omega_f/\omega_c < \omega_f/n\omega_n$ the outer electrons in the swarm are tending to travel with greater than synchronous velocities and can contribute synchronous reactance which masks the effect of changing dielectric constant. The curve for $E/B^2=2$, $r_H/r_c=1.08$ is replotted in Fig. 12 with the effective dielectric constant as given by (23). The expected wavelength shift (with amplitude arbitrarily adjusted to equal the observed shift) is shown by the dotted line. Agreement seems to be good except in the region between $\omega_f/\omega_c=0.575$ and the observed cyclotron resonance. This may be due to the fact that the electrons are approaching synchronous velocities.

The over-all qualitative picture presented by these data is fairly clear, while attention to particular points may be misleading because of experimental inaccuracies or insufficient theoretical understanding. Some of the important conclusions are summarized below, and quantitative results for some particular cases are given in the Appendix.

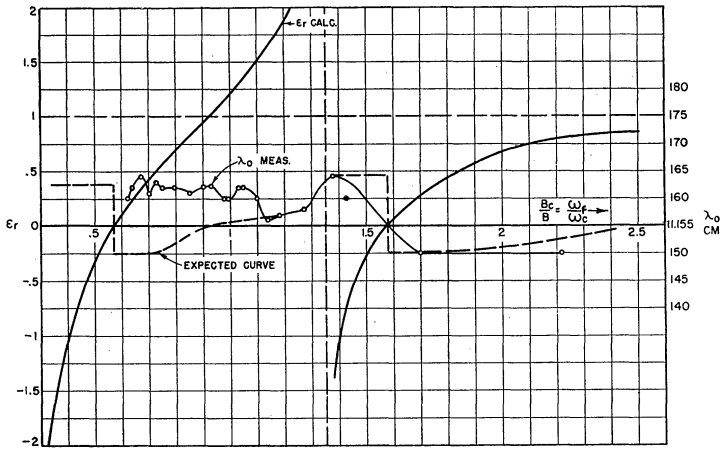

Fig. 12—Effective dielectric constant for magnetron space charge compared with wavelength shift for $r_H/r_c=1.08$.

The three types of effects on frequency are clearly represented by the data.

1. Passive effects due to wave-propagating properties are illustrated as wavelength shift at subsynchronous voltages in Fig. 9 and to the right of the lines $\omega_f/n=\omega_n$ in Fig. 11. The subsynchronous data in Fig. 9(a) illustrate increasing wavelength for $\epsilon_r<0$ and in Fig. 9(d) decreasing wavelength for $0<\epsilon_r<1$. The curves in Fig. 12 which pertain to these effects have been discussed in the last paragraph.

2. Synchronous reactance is demonstrated by the relatively sharp increase in wavelength above synchronous voltage and to the left of the line $\omega_f/n=\omega_n$ in Fig. 11. The case for $E/B^2=5$ is particularly interesting in this connection. The decrease in wavelength showing up in the other curves between $B_c/B=1.05$ and $B_c/B=1.35$ is apparently cancelled by the effects of synchronism. This shows up even more clearly upon careful examination of data of the type shown in Fig. 9 from which this curve was taken. Synchronous reactance will be discussed more completely in the next section.

3. The cyclotron resonance shows up quite obviously in Figs. 9(b), and 9(c), and is, as would be expected, dependent upon anode voltage. It is not clear from the data whether this point is intimately related to the other two effects. It does appear in Fig. 11 that a sharp increase in wavelength with increasing magnetic field should be associated with the cyclotron resonance.

The most probable sources of error are the following:

Magnetic field for the entire series of measurements may be off by 75 to 100 gauss. It is fairly certain that the calibration was not changed during the series of measurements, because it was possible to recheck critical points at the cyclotron resonance and starting voltage.

Dimensions of the magnetron, particularly r_a/r_c, may be in error by 10 to 20 per cent. Another tube which was taken apart had a cathode larger in this proportion. The dimensions used were taken from data in the tube specifications.

Wavelength measurements were made with a Mico wavemeter. The estimated error is ± 0.002 cm. The direction of wavelength shift could always be observed by watching the oscilloscope screen. Determination of the exact resonant wavelength near the cyclotron resonance was difficult because of the distortion of the scope pattern.

Space-Charge Effects in the Oscillating Magnetron

Evidence of space-charge effects in the oscillating magnetron is given in the results of frequency-pushing measurements and in Rieke diagrams. Space-charge effects on frequency in the conventional oscillating tube are of small magnitude, of the order of 1 per cent. Frequency pushing is ordinarily defined as variation of oscillatory frequency with plate current, in contrast with the term frequency pulling, which is, ideally, variation of frequency at constant standing-wave ratio in the Rieke diagram.

More generally it is convenient to think of frequency variation over a performance chart (set of volt ampere characteristics at varying magnetic fields and constant load) and frequency variation with variation in load impedance at constant current and magnetic field as is experienced in the Rieke diagram. Variation of frequency over the performance chart is entirely due to space-charge effects. Variation of frequency in the Rieke diagram is primarily due to changes in the susceptive portion of the load impedance. However, contours of constant frequency in the Rieke load-impedance diagram should follow contours of constant susceptance. The fact that this is not the case may be attributed to space-charge effects.

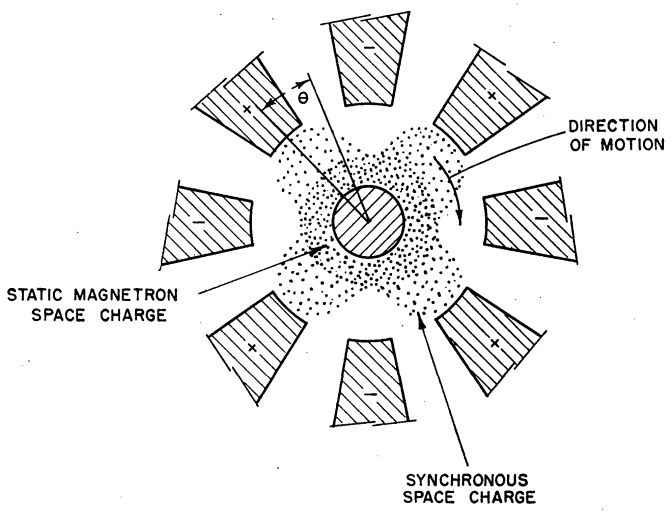

Fig. 13—Pictorial representation of space charge within interaction space.

Fig. 13 presents a qualitative picture of the space-charge swarm with spokes at an instant when the anodes are at their maximum + or − radio-frequency potential. The spokes form on the static magnetron space-charge swarm bounded by the synchronous radius (which can be calculated from (31)). In the nonoscillating magnetron with imposed radio-frequency, as described in the last section, the spokes can form without reaching all the way out to the anode. The maximum radius reached in the spoke is determined by the anode potential, and the spoke will form in the region of the maximum positive potential, 90 electrical degrees ahead of the maximum decelerating field. Thus the current induced by the rotating spokes will lead the radio-frequency voltage by approximately 90 degrees. As the anode potential is increased the spoke will extend farther toward the anode, maintaining the same phase position but increasing the amount of susceptance contributed by the space charge. This accounts for the sharp rise in resonant wavelength before oscillation starts, exhibited in the curves of Figs. 6 through 9. When oscillation starts, the spokes must reach out of the anodes and there is a transport of electrons through the spokes sufficient to supply the dc anode current necessary to provide input power. The generated frequency is usually lower than the frequency of the tank circuit by a margin of the order of $1/Q$. The impedance of the tank circuit is almost a pure inductance and the power delivered from the electron swarm is small. In order for more power to be delivered from the spokes to the circuit the angle θ must be reduced so that the induced current leads the voltage less than 90 degrees. As the voltage is raised further, the phase angle is reduced further, thereby decreasing the positive susceptance contributed by the spokes and decreasing the resonant wavelength. Fig. 6 illustrates this effect. The dotted lines in Fig. 9 also indicate the direction of wavelength shift after oscillation was observed.

The fact that the resonant wavelength does not come back to the cold resonance value may be due to the presence of the hub of subsynchronous space charge. It is important to realize that variation in frequency over the performance chart may depend upon the "passive" effects of the hub of the space-charge wheel as well as the "active" effects of the spokes. Therefore, a complete analysis of pushing data would be more complex than the relatively simple interpretation just given.

The difference in the physical significance of the quantity y_e in the preoscillating and oscillating magnetron as discussed in connection with Fig. 4 is apparent in the above discussion. In the former case, expansion of the hub and synchronous spokes have the major effect, with some complication introduced by the cyclotron resonance. In the latter case, the effect of the hub is probably a constant correction, whereas the phasing of the spokes with respect to the radio-frequency wave in the interaction space makes a major contribution.

Space-charge effects in the Rieke diagram are intimately related to frequency pushing. The rotating swarm is thought of as a current generator, the frequency of which is a function of power output. Power output in turn is a function of the load on the generator. The experimental evidence of Rieke diagrams indicates

the electronic susceptance to be a function of the load conductance on the magnetron. Variation of the conductive portion of the magnetron load without change in the susceptive portion varies the form of the resonance curve without changing its position on the frequency axis. The rotating swarm of electrons must adjust itself to meet the conditions of negative conductance and phase relationship to the radio-frequency voltage imposed by the resonant circuit. In addition, the changing radio-frequency voltage caused by variation in load will react on the electron swarm. This combination of causes must have a very complex, but not very large, effect upon the frequency of oscillation. Further complication results from the fact that a particular value of load conductance (a particular form of the resonance curve) allows maximum efficiency of energy transference from the electron swarm to the radio-frequency field. This is the condition of optimum shunt impedance. The characteristics of the optimum condition are understood for conventional oscillators employing triode or tetrode vacuum tubes, but still not satisfactorily explained in the case of the magnetron oscillator.

Conclusions

The present paper is not meant to be a complete and final analysis of the problem of the magnetron space-charge and frequency characteristics. It is intended to relate as many as possible of the known facts and theories in such a way that it can be used as a guide for further research and development. We have presented in some detail the ideas and data originating in the University of Michigan laboratory and have tried to provide enough discussion and criticism of other ideas to make the development consistent.

Some important conclusions have been mentioned in the discussion of the experimental results and theory. These are the following:

1. Frequency pushing with increasing voltage is primarily due to a decrease in wavelength caused by the active phasing effect of the electrons in the spokes of the space-charge wheel acting as a current generator in the magnetron.

2. The increase in the extent of space-charge spokes as voltage is increased under hot impedance test conditions may also contribute an increasing positive susceptance without change in the phase angle of the spoke relative to the wave of radio-frequency potential.

3. Frequency shifts caused by the subsynchronous swarm as voltage is increased under hot impedance test conditions are primarily of two types. In one case, the dielectric constant of the hub of the space-charge wheel is negative and the resonant wavelength increases as the hub expands. In the other case, the dielectric constant of the hub of the space-charge wheel is positive, but less than unity, and the wavelength decreases as the hub expands. These effects may be called passive effects.

4. For a particular value of magnetic field, under hot impedance test conditions, the natural resonance of the individual electrons in the space charge causes perturbation of the resonant wavelength. This is the cyclotron resonance ($\omega_f = \omega_c$).

5. Frequency pulling is primarily an effect of circuitry. Deviations from the values predicted on the basis of circuitry are due to interrelation of the equivalent susceptance and conductance of the space-charge cloud acting as a current generator in the magnetron. They are therefore related to frequency pushing.

It would be desirable to amplify experience by carrying out experiments designed to determine the exact value of y_e, the electronic admittance, under various conditions in both the nonoscillating and the oscillating cases. Possibly, if enough data were available on different magnetrons, generalizations could be made which would give more insight into the actual behavior in the oscillating magnetron. It is important to realize that, although the frequency shifts due to space-charge effects are small compared to the resonance frequency (of the order of one per cent), an understanding of the underlying causes of these shifts is equivalent to an understanding of the basic electronic principles of magnetron operation.

Frequency shifts of the type mentioned in 3 and 4 above may be used in a reactance tube to produce frequency modulation. The problem of designing a tube of this type has been undertaken in the University of Michigan laboratory. Details of this development will be presented when data are available on operating tubes. Quantitative results and a simple formula, placing limitation on the design of such tubes with multianode structures, are given in the Appendix.

Appendix

The theory and experimental results given in this paper can be used as a basis for design in devices using the magnetron-type space charge to furnish electronic control of frequency. Frequency shifts of the order of 8 per cent of 500 Mc have been obtained using split-anode magnetrons.[7] The space charge may be used within a multianode structure attached to the resonant circuit of the magnetron. The theory which has been developed can be used as a basis for convenient design criteria by which anode structure and interaction space designs can be determined which obtain maximum benefit of the space charge and do not permit oscillation.

In the first place, if we wish to make use of the properties of a space charge of negative dielectric constant, we have the condition

$$\omega_f < 0.36\omega_c. \tag{32}$$

This is obtained from Fig. 2. If we wish to place the

[7] These results were obtained by P. H. Peters at the General Electric Research Laboratories.

further restriction that magnetron does not oscillate, we have the well-known condition

$$B < B_0. \tag{33}$$

If (32) and (33) are combined so that the structure will not oscillate and the space charge will cause total reflection, we obtain the following:

$$\omega_f < 0.36\omega_c = 0.36\,\frac{Be}{m} < 0.36 \times B_0\,\frac{e}{m}$$

$$= 0.36 \times \frac{2\omega_f}{n}\,\frac{1}{1-\dfrac{r_c^2}{r_a^2}}$$

which results in the simple criterion

$$1 - \frac{r_c^2}{r_a^2} < \frac{0.72}{n}$$

or

$$\frac{r_a}{r_c} < \sqrt{\frac{1}{1-0.72/n}}. \tag{34}$$

This last equation gives the following values of r_a/r_c for various values of n:

$n = 1$	$r_a/r_c < 1.88$
2	1.25
3	1.15
4	1.10
5	1.08
6	1.06.

Spacing requirements imposed a limitation on the value of r_a/r_c which can be used and, therefore, on n. For example, if the cathode diameter is of the order of $\frac{1}{2}$ to 1 centimeter, $r_a/r_c < 1.15$ begins to be impractical. Therefore, $N = 2n = 6$ is the largest practical number of anodes. To be on the safe side, $N = 4$ or even $N = 2$ should be used if possible.

If it is desired to make use of the space charge with a positive dielectric constant less than unity the following criterion may be used:

$$\omega_f \gtrsim 1.36\omega_c. \tag{35}$$

ω should not be too much in excess of ω_c; otherwise ϵ_r differs so little from unity that the change in susceptance due to the space charge will not be appreciable. At most, the presence of space charge of these characteristics can do no more than cancel the effect of the cathode. The value of ω_f/ω_c might arbitrarily be limited to less than two for this case. If this is done, we have as before

$$1 - \frac{r_c^2}{r_a^2} < \frac{4}{n}$$

or

$$\frac{r_a}{r_c} < \sqrt{\frac{1}{1-4/n}}. \tag{36}$$

This imposes no serious restriction on r_a/r_c and is actually satisfied in most conventional continuous-wave magnetrons operating at wavelengths greater than 6 centimeters.

The relative merits of these two types of behavior under conditions of high radio-frequency voltage are not yet experimentally determined. On paper the use of space charge of negative dielectric constant can produce an infinite change in λ_0, whereas the space charge of positive dielectric constant can only cancel the effect of the cathode. This latter, of course, can be two to five per cent. The linearity of frequency change and losses under the influence of high radio-frequency voltage might give preference to the latter method. This remains to be seen. The following illustrative cases give quantitative comparison of experimentally observed results with the theory.

The total capacitance in the resonant circuit of any magnetron must include the capacitance between anode and cathode. The latter is the portion which is varied by the presence of the space charge. Let

C_a = total anode-to-anode capacitance including effect of cathode
C_c = total anode-to-cathode capacitance
ΔC_c = change in anode-to-cathode capacitance caused by presence of space-charge swarm.

For a given ΔC_c it can be shown that the resonant wavelength shift is given approximately by

$$\frac{\Delta\lambda_0}{\lambda_0} = \alpha\,\frac{C_c}{C_a}\,\frac{\Delta C_c}{C_c}. \tag{37}$$

Here α is a proportionality factor which is equal to $\frac{1}{2}$ in a lumped-constant circuit since, in this case, wavelength is proportional to the square root of the capacitance. In distributed-constant circuits, as is usually the case in a magnetron, α is less than $\frac{1}{2}$ and must be calculated for the particular case.

C_c/C_a is ordinarily four or five per cent. By particular design it can be made 20 per cent or more.

The method of calculation of $\Delta C_c/C_c$ varies with the geometry and the effective dielectric constant of the space charge. The following two examples are typical.

If $0 < \epsilon_r < 1$ and the space between anode and cathode is just filled by the space-charge swarm (thus having maximum effect),

$$\frac{\Delta C_c}{C_c} = \epsilon_r - 1 \tag{38}$$

where, since ϵ_r is less than unity, the wavelength shift is always negative and the maximum value of shift corresponds to $\Delta C_c/C_c = -1$. In this case the effect of

the cathode is cancelled. Table I gives two sample calculations for this case. ϵ_r is calculated from (23).

In the case of negative ϵ_r, total reflection should occur from the space charge. The cathode diameter is therefore effectively increased by the presence of the space charge. The capacitance between anode and cathode will be a function of the following form:

$$C_c = \frac{K}{\ln r_a/r_c} \tag{39}$$

where K is a function of r_a/r_c because of fringing effects around the anodes. The percentage change in effective capacitance to the cathode is therefore the following, if we consider r_H (radius of the space-charge cloud) as a reflecting surface:

$$\frac{\Delta C_c}{C_c} = \frac{\dfrac{K_H}{\ln r_a/r_H} - \dfrac{K_c}{\ln r_a/r_c}}{\dfrac{K_c}{\ln r_a/r_c}}$$

$$\frac{\Delta C_c}{C_c} = \frac{K_H \log r_a/r_c}{K_c \log r_a/r_H} - 1. \tag{40}$$

Using this result in (37), the following result were obtained in two different tubes constructed in the University of Michigan laboratory. In the second case, a negative dielectric constant is actually not predicted by the theory, but the direction of wavelength shift indicates that the space charge is reflecting. This sort of discrepancy may be due to errors in determination of magnetic field or to the oversimplified nature of the theory.

In the optimum design of a modulator tube, α should be made as large as possible. The second case of Table II illustrates this point. Although a capacitance change of 123 per cent is obtained, due to the small value of α, the wavelength shift is less than one per cent.

Acknowledgments

The author is indebted to all of his co-workers in the University of Michigan Electron Tube Laboratory, particularly to W. G. Dow, who suggested the technique of hot impedance testing, and to J. R. Black, G. R. Brewer, and Miss Rita Callahan, who offered many helpful suggestions and assisted in gathering of experimental information.

TABLE I

Comparison of Theory and Results for $0<\epsilon_r<1$ in the Space-Charge Swarm

E_a volts	B gauss	λ cm	r_a/r_c	r_H/r_c	ω_f/ω_c	C_c/C_a	α	ϵ_r-1 $(\Delta C_c/C_c)$	$\frac{\Delta\lambda_0}{\lambda_0}$ Calculated	$\frac{\Delta\lambda_0}{\lambda_0}$ Observed
190	210	16.85	1.66	1.66	3	0.045	0.5	−0.07	−0.16 per cent	−0.18 per cent
450	450	17.6	1.66	1.66	1.35	0.045	0.5	−1	−2.25 per cent*	−1 per cent

* Note from the solid curve in Fig. 2(a) that ϵ_r is a very critical function of magnetic field in this region so that a 1-per cent error in determined field could produce almost a 100-per cent error in the calculated wavelength shift.

TABLE II

Comparison of Theory and Results for $\epsilon_r<0$ in the Space-Charge Swarm

E_a volts	B gauss	λ cm	r_a/r_c	r_H/r_c	ω_f/ω_c	C_c/C_a	α	$\Delta C_c/C_c$	$\frac{\Delta\lambda_0}{\lambda_0}$ Calculated	$\frac{\Delta\lambda_0}{\lambda_0}$ Observed
1,400	1,700	16.9	1.66	1.11	0.35	0.045	0.5	+0.25	+0.55 per cent	+0.65 per cent
1,400	1,400	13.2	1.33	1.17	0.58	0.05	0.125*	+1.23	+0.77 per cent	+0.76 per cent

* These data were taken on a double-anode modulator tube with a distributed constant circuit—hence the low value of ω. All other data were taken on an interdigital magnetron in which the capacitance was essentially concentrated in the anodes.

DISTRIBUTION LIST

22 copies - Director, Evans Signal Laboratory
Belmar, New Jersey
FOR - Chief, Thermionics Branch

12 copies - Chief, Bureau of Ships
Navy Department
Washington 25, D. C.
ATTENTION: Code 930A

12 copies - Director, Air Materiel Command
Wright Field
Dayton, Ohio
ATTENTION: Electron Tube Section

4 copies - Chief, Engineering and Technical Service
Office of the Chief Signal Officer
Washington 25, D. C.

2 copies - H. Wm. Welch, Jr., Research Physicist
Electron Tube Laboratory
Engineering Research Institute
University of Michigan
Ann Arbor, Michigan

1 copy - Engineering Research Institute File
University of Michigan
Ann Arbor, Michigan

W. E. Quinsey, Assistant to the Director
Engineering Research Institute
University of Michigan
Ann Arbor, Michigan

W. G. Dow, Professor
Department of Electrical Engineering
University of Michigan
Ann Arbor, Michigan

Gunnar Hok, Research Engineer
Engineering Research Institute
University of Michigan
Ann Arbor, Michigan

J. R. Black, Research Engineer
Engineering Research Institute
University of Michigan
Ann Arbor, Michigan

G. R. Brewer, Research Associate
Engineering Research Institute
University of Michigan
Ann Arbor, Michigan

J. S. Needle, Instructor
Department of Electrical Engineering
University of Michigan
Ann Arbor, Michigan

Department of Electrical Engineering
University of Minnesota
Minneapolis, Minnesota
ATTENTION: Professor W. G. Shepherd

Westinghouse Engineering Laboratories
Bloomfield, New Jersey
ATTENTION: Dr. J. H. Findlay

Columbia Radiation Laboratory
Columbia University
Department of Physics
New York 27, New York

Electron Tube Laboratory
Department of Electrical Engineering
University of Illinois
Urbana, Illinois

Department of Electrical Engineering
Stanford University
Stanford, California
ATTENTION: Dr. Karl Spangenberg

National Bureau of Standards Library
Room 203, Northwest Building
Washington 25, D. C.

Radio Corporation of America
RCA Laboratories Division
Princeton, New Jersey
ATTENTION: Mr. J. S. Donal, Jr.

Department of Electrical Engineering
The Pennsylvania State College
State College, Pennsylvania
ATTENTION: Professor A. H. Waynick

Document Office - Room 20B-221
Research Laboratory of Electronics
Massachusetts Institute of Technology
Cambridge 39, Massachusetts
ATTENTION: John H. Hewitt

Bell Telephone Laboratories
Murray Hill, New Jersey
ATTENTION: S. Millman

Special Development Group
Lancaster Engineering Section
Radio Corporation of America
RCA Victor Division
Lancaster, Pennsylvania
ATTENTION: Hans K. Jenny

Magnetron Development Laboratory
Power Tube Division
Raytheon Manufacturing Company
Waltham 54, Massachusetts
ATTENTION: Edward C. Dench

Vacuum Tube Department
Federal Telecommunication Laboratories, Inc.
500 Washington Avenue
Nutley 10, New Jersey
ATTENTION: A. K. Wing, Jr.

Microwave Research Laboratory
University of California
Berkeley, California
ATTENTION: Professor L. C. Marshall

General Electric Research Laboratory
Schenectady, New York
ATTENTION: Dr. A. W. Hull

General Electric Research Laboratory
Schenectady, New York
ATTENTION: P. H. Peters

Cruft Laboratory
Harvard University
Cambridge, Massachusetts
ATTENTION: Professor E. L. Chaffee

Research Laboratory of Electronics
Massachusetts Institute of Technology
Cambridge, Massachusetts
ATTENTION: Professor S. T. Martin

Collins Radio Company
Cedar Rapids, Iowa
ATTENTION: Robert M. Mitchell

Department of Electrical Engineering
University of Kentucky
Lexington, Kentucky
ATTENTION: Professor H. Alexander Romanowitz

Department of Electrical Engineering
Yale University
New Haven, Connecticut
ATTENTION: Dr. H. J. Reich

Department of Physics
Cornell University
Ithaca, New York
ATTENTION: Dr. L. P. Smith

Document Office for Government Research Contracts
Harvard University
Cambridge, Massachusetts
ATTENTION: Mrs. Marjorie L. Cox

Mr. R. E. Harrell
West Engineering Library
University of Michigan
Ann Arbor, Michigan

Mr. C. L. Cuccia
RCA Laboratories Division
Radio Corporation of America
Princeton, New Jersey

Dr. O. S. Duffendack, Director
Phillips Laboratories, Inc.
Irvington-on-Hudson, New York

Air Force Cambridge Research Laboratories
Library of Radiophysics Directorate
230 Albany Street
Cambridge, Massachusetts

Air Force Cambridge Research Laboratories
Library of Geophysics Directorate
230 Albany Street
Cambridge, Massachusetts
ATTENTION: Dr. E. W. Beth